Available online at www.sciencedirect.com
ScienceDirect
Journal of Sound and Vibration 304 (2007) 556–569
JOURNAL OF SOUND AND VIBRATION
www.elsevier.com/locate/jsvi

# A technique for overcoming load discontinuity in using Newmark method

Shuenn-Yih Chang*

*Department of Civil Engineering, National Taipei University of Technology, NTUT Box 2653, No. 1, Section 3, Jungshiau East Road, Taipei 106-08, Taiwan, Republic of China*

Received 4 January 2005; received in revised form 1 March 2007; accepted 2 March 2007

**Abstract**

Although a closed form solution can be obtained for the shock response to an impulse by using the Duhamel integral method for a single degree-of-freedom system, it is analytically verified herein that an extra amplitude distortion will be introduced at the end of the impulse by using the Newmark method. In fact, the relative amplitude error in the displacement response due to the discontinuity at the end of the impulse can be reliably estimated by the ratio of the area of extra impulse over the area of input impulse, where the area of extra impulse is equal to a half of the product of the time step and load discontinuity. It seems that the momentum equation of motion can be used to easily overcome the discontinuity problem at the end of an impulse. This is because the external force is replaced by its corresponding external momentum, which is obtained from the time integration of external force, and thus the discontinuity problem automatically disappears by using the momentum equation of motion. Numerical studies reveal that this technique is applicable to nonlinear systems. Meanwhile, it is also numerically illustrated that the discontinuity problem can be overcome by performing a very small time step immediately upon termination of the applied impulse.


## 1. Introduction

Mathematical expressions to define the dynamic displacements are the equations of motion of a structure, and solutions of these equations of motion give the desired displacement time history. The mathematical formulation of equations of motion for a dynamic system might be the most important and sometimes the most difficult phase of the entire dynamic analysis procedure. The ***d'Alembert's principle*** provides the concept that a mass develops an inertial force proportional to its acceleration and opposing it [1,2]. Therefore, it is convenient to express equations of motion as equations of dynamic equilibrium, which consists of the four types of forces acting on the structure. In general, these are elastic constraints which oppose displacements, viscous damping forces which resist velocities, inertial forces which resist accelerations and independently defined external forces. Thus, the external force must be accurately represented so that a reliable solution can be obtained.

*Tel.: +886 2 2771 2171x2653; fax: +886 2 2781 4518.
*E-mail address:* changsy@ntut.edu.tw.

0022-460X/$ - see front matter 
doi:10.1016/j.jsv.2007.03.032

In the time history analysis, the external force may be a very rapidly changing function of time. Hence, a very small time, which may be much smaller than that required by accuracy consideration, is required to accurately represent the external force so that reliable solutions can be achieved. This difficulty can be effectively overcome by using the integrated equation of motion to smooth out the rapid changes of dynamic loading [3,4]. Meanwhile, in the step-by-step solution of the response to an impulse, a very small time step, which might be much smaller than the duration of the impulse and/or that required by accuracy consideration, is generally needed to yield a reliable solution. It will be shown that the discontinuity at the end of the impulse is responsible for this difficulty if the Newmark method is used. Since this discontinuity disappears after utilizing the time integration, the integrated equation of motion seems very promising. In addition, the maximum displacement response to an impulse depends principally upon the magnitude of the applied impulse and is not strongly affected by the form of the impulse. Both imply that the use of ***the principle of impulse and momentum*** to develop a governing equation is promising. In fact, the dynamic equilibrium of spring, damping, inertial and external momentums acting on the system lead to the momentum equation of motion. This derivation is similar to that of the conventional form of equation of motion, which is referred to as the force equation of motion herein. However, the basic component "**force**" is replaced by the "**momentum**". A simple way is used to prove that the discontinuity at the end of impulse will result in a displacement error by using the Newmark method and a reliable way to estimate the relative amplitude error is presented. It is also shown that this discontinuity disappears on using the momentum equation of motion. Analytical results are confirmed by numerical examples.

## 2. Equation of motion

The equation of motion for a structural system is formulated based on the dynamic equilibrium of force, which includes four types of forces that include the elastic spring resisting force, damping resisting force, inertial resisting force and external force. A schematic sketch of such an idealized single degree-of-freedom system is shown in Fig. 1, and its force free-body diagram is depicted in Fig. 2. As a result, the equation of motion for the system can be derived from the dynamic equilibrium of the four types of force acting on it and has the following expression:

$$f_I + f_D + f_S = f_E, \tag{1}$$

where

$$\begin{aligned} f_I &= m\ddot{u}(t) = \text{inertial force}, \\ f_D &= c\dot{u}(t) = \text{damping force}, \\ f_S &= ku(t) = \text{spring force}, \\ f_E &= f(t) = \text{external force}, \end{aligned} \tag{2}$$

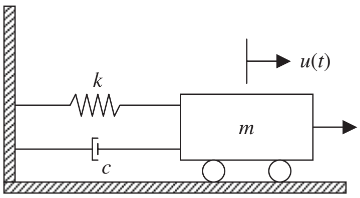


Fig. 1. Idealized single degree-of-freedom system.

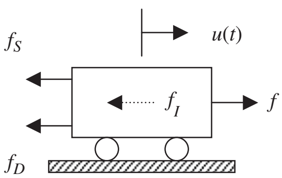


Fig. 2. Dynamic equilibrium of forces.

in which $m$ is the mass, $c$ the viscous damping coefficient, $k$ the stiffness and $f$ the external force; $\ddot{u}(t)$, $\dot{u}(t)$ and $u(t)$ are the displacement, velocity and acceleration, respectively. After substituting Eq. (2) into Eq. (1), it becomes

$$m\ddot{u}(t) + c\dot{u}(t) + ku(t) = f(t). \tag{3}$$

The initial value problem for this equation of motion is to find a solution $u(t)$ having the given initial conditions of $u(0) = u_0$ and $\dot{u}(0) = \dot{u}_0$.

Since the maximum displacement response to an impulse depends principally upon the total amount of the applied impulse (external momentum) [1,2] and is almost unaffected by the form of the loading impulse, it is very promising to solve this problem by considering the external momentum directly. Therefore, there is a great motivation to construct the governing equation of motion from the dynamic equilibrium of momentums, which involves using external momentum in the formulation. The free-body diagram to describe dynamic equilibrium of momentums corresponding to the single degree-of-freedom system defined in Fig. 1 is plotted in Fig. 3 and the governing equation of motion for the free-body diagram can be written as

$$M_I + M_D + M_S = M_E, \tag{4}$$

where

$$\begin{aligned} M_I &= \int_0^t F_I(\tau)\mathrm{d}\tau = \int_0^t m\ddot{u}(\tau)\mathrm{d}\tau = \text{inertial momentum}, \\ M_D &= \int_0^t F_D(\tau)\mathrm{d}\tau = \int_0^t c\dot{u}(\tau)\mathrm{d}\tau = \text{damping momentum}, \\ M_S &= \int_0^t F_S(\tau)\mathrm{d}\tau = \int_0^t ku(\tau)\mathrm{d}\tau = \text{spring momentum}, \\ M_E &= \int_0^t F_E(\tau)\mathrm{d}\tau = \int_0^t f(\tau)\mathrm{d}\tau = \text{external momentum}. \end{aligned} \tag{5}$$

In general, $m$, $c$ and $k$ are constant for a linear elastic system and the result of Eq. (5) is

$$\begin{aligned} M_I &= m\dot{u}(t) - m\dot{u}(0), \\ M_D &= cu(t) - cu(0), \\ M_S &= k\bar{u}(t) - k\bar{u}(0), \\ M_E &= \bar{f}(t) - \bar{f}(0). \end{aligned} \tag{6}$$

After the substitution of Eq. (6) into Eq. (4), the explicit expression of Eq. (4) is

$$m\dot{u}(t) + cu(t) + k\bar{u}(t) - \bar{f}(t) = m\dot{u}(0) + cu(0) + k\bar{u}(0) - \bar{f}(0). \tag{7}$$

It is reasonable to assume that the dynamic equilibrium of momentums is satisfied at the beginning of motion. This implies that the momentum equation of motion is satisfied at the time of $t = 0$, i.e., $m\dot{u}(0) + cu(0) + k\bar{u}(0) = \bar{f}(0)$. As a result, Eq. (7) is reduced to be

$$m\dot{u}(t) + cu(t) + k\bar{u}(t) = \bar{f}(t), \tag{8}$$

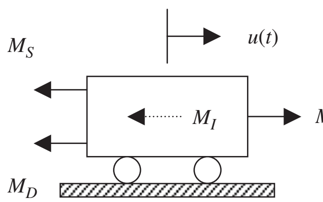


Fig. 3. Dynamic equilibrium of momentums.

where

$$\bar{u}(t) = \int_0^t u(\tau)\mathrm{d}\tau, \quad \bar{f}(t) = \int_0^t f(\tau)\mathrm{d}\tau. \tag{9}$$

Apparently, $\bar{u}(t)$ is the integral of displacement with respect to time once and $\bar{f}(t) = M_E$ is the external momentum. Unlike using the dynamic equilibrium of momentums to develop Eq. (8), it can be derived by integrating Eq. (3) with respect to time once [3,5].

## 3. Step-by-step solution of shock response

To obtain an analytical solution of the equation of motion is almost impossible if the external force varies arbitrarily with time or the system is nonlinear. It seems the step-by-step integration method is the most powerful technique to solve such problems. The Newmark method [6] is very commonly used in the solution of initial value problems and has the general formulation of

$$\begin{aligned} &ma_{i+1} + cv_{i+1} + kd_{i+1} = f_{i+1}, \\ &d_{i+1} = d_i + (\Delta t)v_i + (\Delta t)^2\left[\left(\frac{1}{2} - \beta\right)a_i + \beta a_{i+1}\right], \\ &v_{i+1} = v_i + (\Delta t)[(1-\gamma)a_i + \gamma a_{i+1}], \end{aligned} \tag{10}$$

where $d_i$, $v_i$, and $a_i$ are the approximate solutions of the displacement, velocity and acceleration, respectively, and $f_i = f(t = t_i)$. The subscript $i$ denotes the time step at $t = t_i = i(\Delta t)$. Numerical characteristics of this family of the Newmark methods are mainly controlled by the parameters $\beta$ and $\gamma$. On the other hand, the Newmark method can be also applied to solve the momentum equation of motion as shown in Eq. (8). However, slight modifications are needed. In general, it can be expressed as

$$\begin{aligned} &mv_{i+1} + cd_{i+1} + ks_{i+1} = \bar{f}_{i+1}, \\ &s_{i+1} = s_i + (\Delta t)d_i + (\Delta t)^2\left[\left(\frac{1}{2} - \beta\right)v_i + \beta v_{i+1}\right], \\ &d_{i+1} = d_i + (\Delta t)[(1-\gamma)v_i + \gamma v_{i+1}], \end{aligned} \tag{11}$$

where $s_i$ is the approximation to the time integral of the displacement of $\bar{u}(t_i)$ for the $i$th time step . The first line of this equation reveals that the external momentum is directly inputted into the system.

## 4. Shock response to point load

In order to analytically prove that the discontinuity in the external force will result in an extra displacement by using the Newmark method while there is no discontinuity in the corresponding external momentum and thus no extra displacement, the shock response to a point load is obtained from both the force equation of motion and the momentum equation of motion. Although viscous damping is included in the force and momentum equations of motion as shown in Eqs. (3), (8), (10) and (11) for completeness, it is generally not considered in computing the shock response to an impulse. This is because damping has much less importance in controlling the maximum response of a system to an impulse than for harmonic or periodic loads since the maximum response to an impulse will be reached in a very short time, before the damping force can absorb much energy from the system [1,2]. Hence, viscous damping is excluded in this study of impulse.

### 4.1. Force equation of motion

Fig. 4(a) shows a point load with the magnitude of $q$ at the time of $t = 0$. Apparently, the displacement response to this point load is theoretically found to be zero, since the point load leads to a zero external momentum as shown in Fig. 4(b). This is because that the point load has a finite magnitude with an infinitely small duration. However, the displacement response to the point load is nonzero if it is computed from a step-by-step integration method. In fact, it can be computed from Eq. (10) for the initial data of $d_0 = v_0 = 0$ and $f_0 = q$. At first, $a_0 = q/m$ is obtained from the equation of motion. Using the first line of Eq. (10), it is found that $a_1 = -(k/m)d_1$ as $f_1 = 0$. Thus, the displacement response $d_1$ can be computed from the second line of Eq. (10) after the substitutions of $a_0$ and $a_1$ with $d_0 = v_0 = 0$ into it and the result is found to be

$$d_1 = E_{\mathrm{dcn}}\left(\frac{q}{k}\right) \text{ where } E_{\mathrm{dcn}} = \frac{(\frac{1}{2} - \beta)\Omega^2}{1 + \beta\Omega^2}, \tag{12}$$

where $\Omega = \omega(\Delta t)$ and $\omega = \sqrt{k/m}$ is the natural frequency of the system, and $E_{\mathrm{dcn}}$ represents the error amplification factor for discontinuity. This result reveals that the displacement response to the point load is nonzero on using the Newmark method. This is because that the value of $q$ is the input external force at the beginning and then an extra impulse of $q(\Delta t)/2$, which is represented by the shaded area shown in Fig. (4a), is introduced into the system. Hence, an extra displacement is generated subsequently.

It is clear that the extra impulse and the extra displacement are closely related to the magnitude of the discontinuity in external force $q$ and the integration time step $\Delta t$. Furthermore, a different member of the Newmark method might lead to a different extra displacement for the same extra impulse, since the displacement $d_1$ is a function of $\beta$. In order to show the difference for different members, variations of the error amplification factors for discontinuity $E_{\mathrm{dcn}}$ with $\Omega$ are plotted in Fig. 5 for the Newmark explicit method ($\beta = 0$), the Fox–Goodwin method ($\beta = \frac{1}{12}$), the linear acceleration method ($\beta = \frac{1}{6}$), the constant average acceleration method ($\beta = \frac{1}{4}$) and the trapezoidal rule with $\beta = \frac{1}{2}$. In this figure, it is found that the error amplification factor generally increases with the increase of $\Omega$ for each method except for the trapezoidal rule with $\beta = \frac{1}{2}$, since its error amplification error is always equal to zero for any positive value of $\Omega$. Meanwhile, it decreases with the increase of the value of $\beta$ for a given value of $\Omega$. This implies that, among the five integration methods, the Newmark explicit method will result in the largest displacement error due to the discontinuity in external force while the trapezoidal rule with $\beta = \frac{1}{2}$ leads to no displacement error. Although the five integration methods, in general, have different error amplification factors for a given value of $\Omega$ these

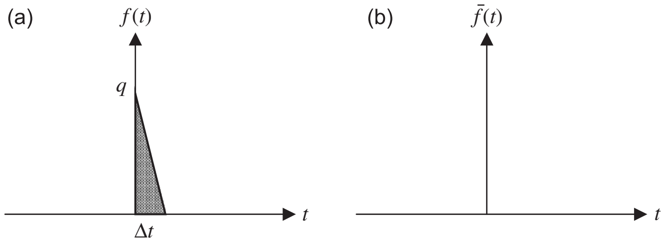


Fig. 4. Point load and its time integral: (a) nonzero external force and (b) zero external momentum.

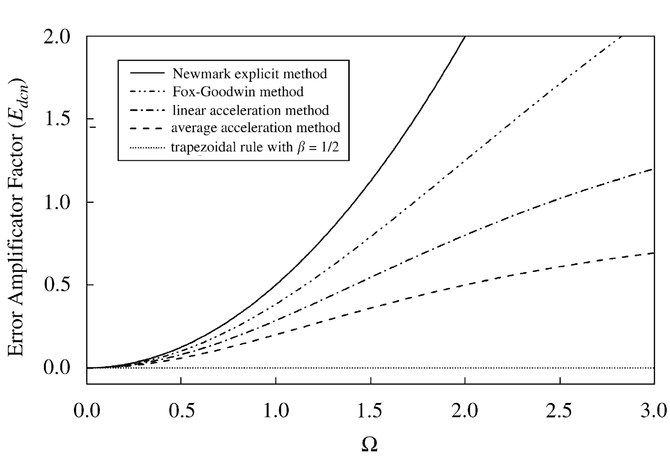


Fig. 5. Variations of error amplification factor for discontinuity $E_{\mathrm{dcn}}$ with $\Omega$.

factors are small for a small value of $\Omega$. On the other hand, since all modal responses are important for the shock response to impulse, an accurate integration of each mode entails the use of a small time step and thus the value of $\Omega$ is small for each mode. Consequently, for small $\Omega$, the difference in error amplification factor among the members of the Newmark method is insignificant except for the trapezoidal rule with $\beta = \frac{1}{2}$, since it has a zero error amplification factor for any positive value of $\Omega$.

### 4.2. Momentum equation of motion

Fig. 4(b) shows that the area of the point load tends to zero since it has a finite magnitude with an infinitely small duration. Therefore, the displacement response obtained from using the Newmark method to solve the momentum equation of motion as shown in Eq. (11) is zero for the initial data of $d_0 = v_0 = 0$ and $\bar{f}_0 = 0$. This implies that there is no discontinuity in the external momentum and thus no extra displacement response if the step-by-step solution of the shock response to the point load is obtained from solving the momentum equation of motion.

## 5. Shock response to arbitrary impulse

A closed form solution for the shock response to an arbitrary impulse can be found from the Duhamel integral [1,2] and is

$$u(t) = \left(\frac{1}{m\omega}\right) \int_0^t f(\tau)\, \sin(t - \tau)\mathrm{d}\tau, \tag{13}$$

where $\omega$ is the natural frequency of the system and $f(\tau)$ the impulse. Thus, the discontinuity problem is caused by the choice of time step and the choice of $\beta$ if using the Newmark method to solve the equation of motion. In fact, the above study reveals that the discontinuity at the end of an impulse will lead to an extra impulse and thus an extra displacement in the step-by-step integration. It is found from the fundamental theory of structural dynamics that the maximum displacement response to impulse is almost proportional to the magnitude of the applied impulse and is not strongly influenced by the form of the impulse. Thus, the relative displacement error arising from the extra impulse is the ratio of the area of the extra impulse over the area of the input impulse. A schematic sketch for computing the relative amplitude error is shown in Fig. 6(a). In fact, it is estimated by

$$E_{\mathrm{est}} = \frac{A_{\mathrm{ext}}}{A_{\mathrm{inp}}}, \quad A_{\mathrm{ext}} = \frac{1}{2} q(\Delta t), \tag{14}$$

where $A_{\mathrm{inp}}$ and $A_{\mathrm{ext}}$ are the area of the input impulse and the extra impulse, respectively. It should be mentioned that the estimation of the relative amplitude error $E_{\mathrm{est}}$ is very accurate for the shock response to impulse. This might be explained by two considerations. First, it is manifested from Eq. (12) or Fig. 5 that the extra displacement response is almost proportional to $q$ and $\Delta t$ for a small $\Omega$. Secondly, the value of $\Omega$ is always very small for accurate integration of a shock response. This is because for an impulse, the loading time

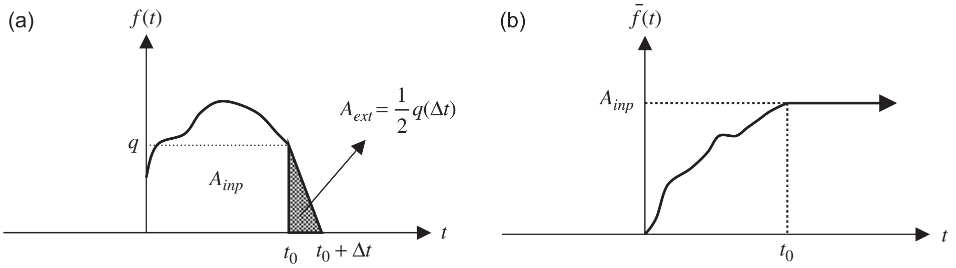


Fig. 6. Arbitrary impulse and its time integral: (a) discontinuity at end of external force and (b) no discontinuity at end of external momentum.

$t_0$ is required to satisfy $t_0/T \leqslant \frac{1}{4}$. Furthermore, the time step $\Delta t$ must be smaller than $t_0$ in order to have an accurate representation of the impulse.

Fig. 6(b) shows the external momentum, which is the result of the time integration of the arbitrary impulse as shown in Fig. 6(a). This figure reveals that the external momentum becomes a constant after the loading duration and there is no discontinuity in the external momentum at the time $t_0$. It is apparent that the constant external momentum is equal to the total amount of the impulse. This implies that a time step larger than the loading duration $t_0$ may still lead to a reliable solution since the total amount of the impulse is inputted into the system in the step-by-step solution of momentum equation of motion. This phenomenon is named an external momentum-dependent effect herein.

## 6. Numerical verifications

In these numerical verifications, the shock responses to three different shapes of impulses for a single degree-of-freedom system and those to a triangular ground impulse for a 5-story structure are obtained from the Newmark method. These results are used to confirm that

(1) The discontinuity at the end of an impulse will lead to an extra displacement error if the force equation of motion is used, while this error disappears if the momentum equation of motion is used, since there is no discontinuity in external momentum. The external momentum-dependent effect for the momentum equation of motion is also verified.
(2) The relative amplitude error caused by the discontinuity at the end of an impulse can be reliably estimated by Eq. (14).
(3) The displacement response errors obtained from different members of the Newmark method are insignificant for the response to impulse since the value of $\Omega$ is small.
(4) The discontinuity of external force can be eliminated by performing a very small single time step right after the end of the discontinuity while using much larger time step subsequently.
(5) The momentum equation of motion is also applicable for nonlinear systems.

It should be mentioned that to avoid the difficulty arising from linearization errors [7–10], linear elastic systems are generally considered in this numerical study. In addition, the solution theoretically obtained is considered as an "**exact**" solution for comparison for linear elastic analysis. However, Example 4 is employed to show that the numerical characteristics are also preserved for nonlinear systems.

### *6.1. Example 1*

An undamped single degree-of-freedom system subject to three different shapes of impulses, which are in the shapes of descending triangle, rectangle and rising triangle, are considered. The lumped mass and stiffness of the system are taken as 1 kg and $\pi^2$ N/m, respectively. These lead to a period of 2 s for the system. The shape of each impulse $f(t)$ and its external momentum $\bar{f}(t)$ for the three impulses are shown in Fig. 7. In each plot, the external momentum is the resultant of the time integration of the impulse. To satisfy the requirement of $t_0/T \leqslant \frac{1}{4}$ for an impulse [1,2] the loading duration $t_0$ is chosen to be 0.05 s, which leads to $t_0/T = \frac{1}{40}$ for the three impulses. In addition, the amplitude is appropriately specified for each impulse in order to have exactly the same external momentum for the three impulses. It is found that the shapes of the three impulses vary significantly with time. However, differences in the three shapes of the external momentums are insignificant in the forced vibration phase and the same external momentum is found in the free vibration phase. The external force is zero after loading duration while it becomes a constant for the external momentum. Apparently, the discontinuity in the rectangular and rising triangular impulses is no longer found after the time integration of these impulses.

The Newmark explicit method is used to solve the force and momentum equations of motion. For brevity, Scheme (a) denotes the use of Newmark explicit method to solve the force equation of motion while the momentum equation of motion solved by this method is referred to as Scheme (b). Four time steps, which are $\Delta t = 0.005$, 0.025, 0.05 and 0.1 s, are used for the step-by-step integration. Thus, the ratios of $\Delta t/t_0$ are found

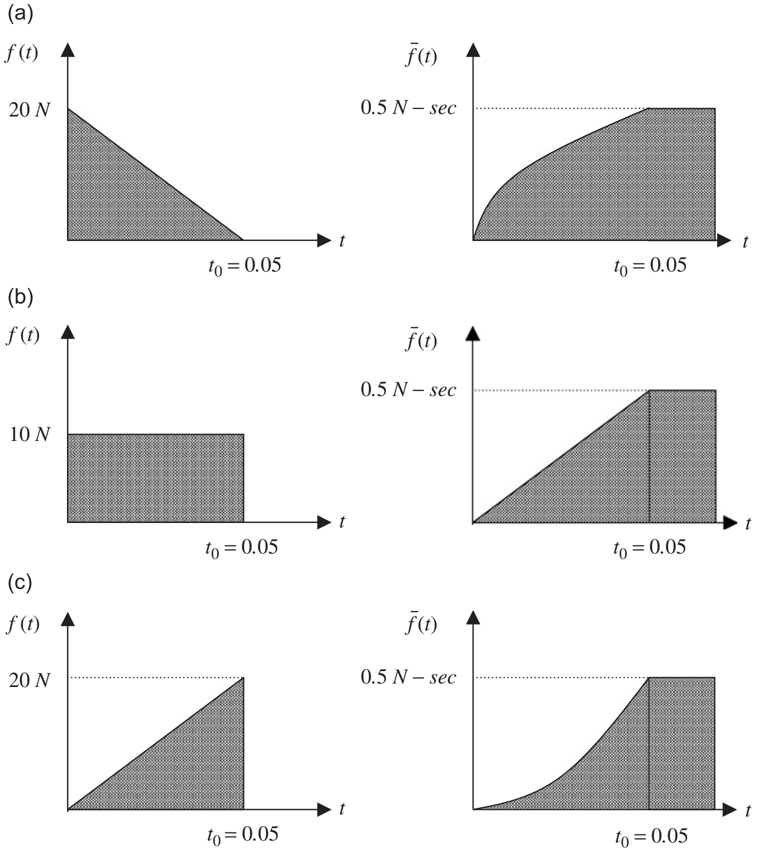


Fig. 7. Three different impulses and their corresponding external momentums: (a) half sine-wave impulse, (b) rectangular impulse and (c) triangular impulse.

to be $\frac{1}{10}$, $\frac{1}{2}$, 1 and 2, and, the ratios of $\Delta t/T$ are found to be $\frac{1}{400}$, $\frac{1}{80}$, $\frac{1}{40}$ and $\frac{1}{20}$, where $T$ is the period of the system and is equal to 2 s. This implies that accuracy consideration is unnecessary since the ratios of $\Delta t/T$ are so small and thus almost no period distortion is introduced. Schemes (a) and (b) are used to compute the responses to the three impulses, and the displacement response errors, which are the differences between the numerical and theoretical solutions, and are depicted in Figs. 8–10.

In Fig. 8, the displacement errors for using Scheme (a) with $\Delta t/t_0 = \frac{1}{10}, \frac{1}{2}$, and 1 are very small, while those in Figs. 9 and 10 are much larger and these errors are increased with the increase of time step. This is because the descending triangular impulse has no discontinuity at its end while the discontinuity is found at the end of the rectangular and rising triangular impulses. It is apparent that the increase of displacement error with an increasing time step is because the extra impulse is proportional to the size of time step. On the other hand, the displacement errors for using Scheme (b) with $\Delta t/t_0 = \frac{1}{10}, \frac{1}{2}$ and 1 are very small for the three impulses. No discontinuity in the three external momentums is responsible for the very small errors. It is very interesting to find that for $\Delta t/t_0 = 2$, Scheme (b) always provides reliable solutions, while Scheme (a) gives inaccurate solutions except for the shock response to the rectangular impulse. This can be explained next. An accurate shock response can be obtained if the total amount of the impulse is considered. Apparently, this amount is the constant external momentum after the loading duration and is entirely taken into account by using Scheme (b), although a time step used is larger than the loading duration. However, it is almost impossible for Scheme (a) to capture the total amount of an impulse if a time step larger than the loading duration is used. In this example, the total amount of impulse considered for the descending triangular impulse, rectangular impulse and the rising triangular impulse is 1, 0.5 and 0 N s, respectively. Since the correct amount should be of 0.5 N s, this thoroughly explains why Scheme (a) with $\Delta t/t_0 = 2$ gives reliable solutions for the rectangular impulse

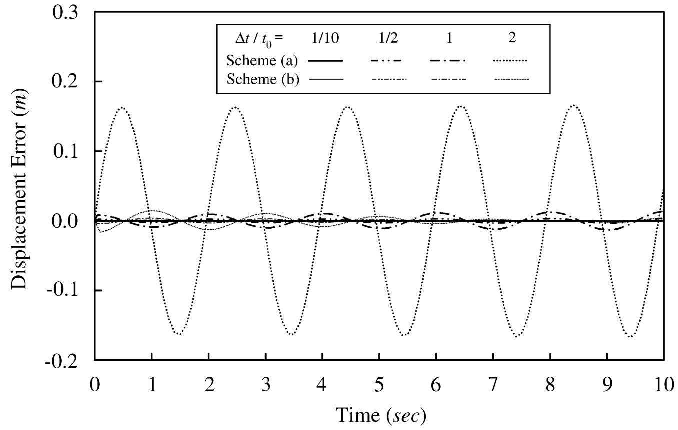


Fig. 8. Displacement error for response to descending triangle impulse.

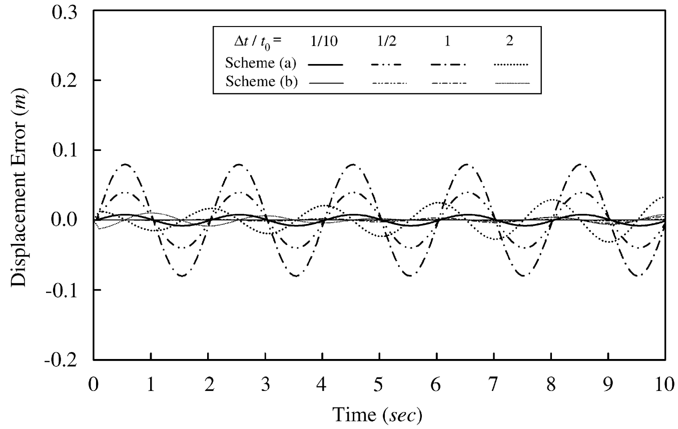


Fig. 9. Displacement error for response to rectangular impulse.

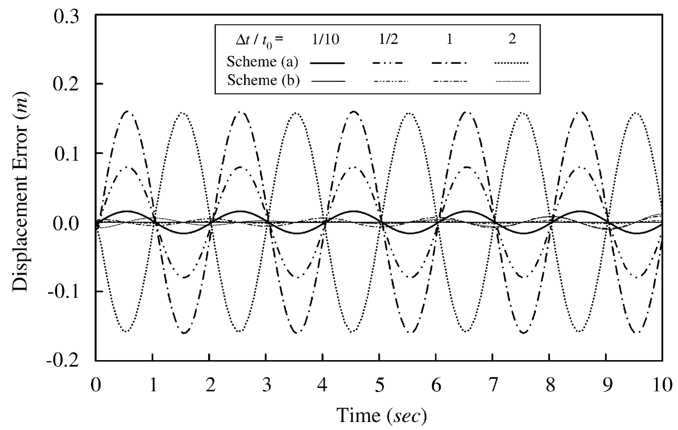


Fig. 10. Displacement error for response to rising triangle impulse.

while it provides inaccurate solutions for the two other impulses. This confirms that the momentum equation of motion can effectively reflect the external momentum-dependent effect although the time step used is larger than the loading duration.

In order to confirm the reliability of Eq. (14), the estimated and actual relative amplitude errors are listed in Table 1 for the three impulses with $\Delta t = 0.005$, 0.025, 0.05 and 0.1. In this table, $E^a_{act}$ and $E^b_{act}$ represent the actual relative amplitude errors on using Schemes (a) and (b), respectively, while $E_{est}$ denotes the estimated relative amplitude error by using Eq. (14). It is found that $E^a_{act}$ is generally consistent with $E_{est}$ except for the rising triangular impulse with a time step of $\Delta t = 0.1$ s. This is because the starting and ending points, both which are zero for this time step and thus a zero response is found. This consistency implies that the relative amplitude error caused by the discontinuity at the end of an impulse can be reliably estimated by Eq. (14). The slight difference in the descending triangular impulse for $\Delta t = 0.1$ and that in the rising triangular impulse for $\Delta t = 0.05$ might be due to the loss of the peak displacement by using a large time step. However, it should be mentioned that $E^b_{act} = 0$ for the three impulses with $\Delta t = 0.005$, 0.025, 0.05 and 0.1 implies the total amount of each impulse is exactly inputted into the system and thus an accurate shock response is achieved.

### 6.2. Example 2

To confirm that the shock response to impulse is insignificant to the use of a different member of the Newmark method except for the trapezoidal rule with $\beta = \frac{1}{2}$, the system used in example 1 is also considered in this example. In fact, the Newmark explicit method, Fox–Goodwin method, linear acceleration method, constant average acceleration method and the trapezoidal rule with $\beta = \frac{1}{2}$ are applied to solve the force equation of motion to obtain the shock response to the rising triangular impulse. The time step of $\Delta t = 0.05$ is used in all computations. Displacement errors are shown in Fig. 11. It is apparent that the displacement errors are almost the same for the Newmark explicit method, Fox–Goodwin method, linear acceleration method and constant average acceleration method, while those for the trapezoidal rule with $\beta = \frac{1}{2}$ are much smaller. This can be explained by next example. For this time step, the very small value of $\Omega$ is 0.157 and thus the error amplification factors of discontinuity for the Newmark explicit method, Fox–Goodwin method, linear acceleration method and constant average acceleration method are 1.2%, 1.0%, 0.8% and 0.6%, respectively.

Table 1
Comparisons of relative amplitude errors

| Shape $\Delta t$ | Descending triangular impulse | | | Rectangular impulse | | | Rising trianguar impulse | | |
|---|---|---|---|---|---|---|---|---|---|
| | $E^a_{act}$ | $E^b_{act}$ | $E_{est}$ | $E^a_{act}$ | $E^b_{act}$ | $E_{est}$ | $E^a_{act}$ | $E^b_{act}$ | $E_{est}$ |
| 0.005 | 0.00 | 0.00 | 0.00 | 0.05 | 0.00 | 0.05 | 0.10 | 0.00 | 0.10 |
| 0.025 | 0.00 | 0.00 | 0.00 | 0.25 | 0.00 | 0.25 | 0.50 | 0.00 | 0.50 |
| 0.050 | 0.00 | 0.00 | 0.00 | 0.50 | 0.00 | 0.50 | 0.98 | 0.00 | 1.00 |
| 0.100 | 1.03 | 0.00 | 1.00 | 0.01 | 0.00 | 0.00 | −1.00 | 0.00 | N.A |

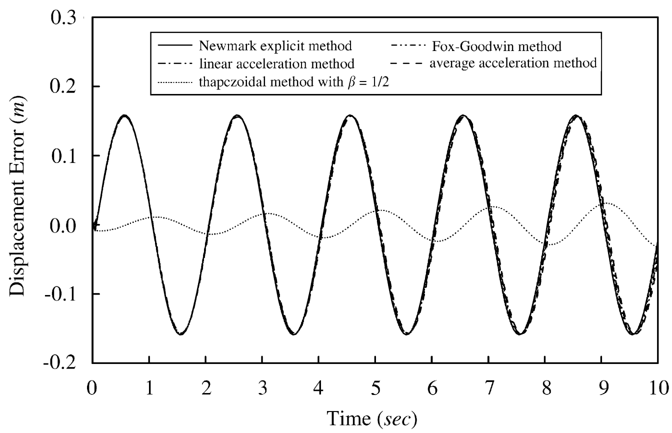


Fig. 11. Shock response from different members of Newmark method.

Hence, commensurate displacement errors are found. On the other hand, a zero error amplification factor is responsible for the smallest errors for the trapezoidal rule with $\beta = \frac{1}{2}$. It should be mentioned that the displacement error for using the trapezoidal rule with $\beta = \frac{1}{2}$ is not exactly equal to zero since a slight period distortion is introduced for $\Delta t = 0.05$. This time step is the largest time step, which is equal to the loading duration, to solve the force equation of motion. These results confirm that the displacement response error caused by the discontinuity at the end of an impulse is insignificant to the member of the Newmark method used for step-by-step integration except for the trapezoidal rule with $\beta = \frac{1}{2}$.

### 6.3. Example 3

Since the extra impulse is proportional to the time step, the discontinuity problem might be eliminated by performing a very small single time step right after the end of the impulse while using much larger time step subsequently. In order to illustrate this scheme, the system used in example 1 is employed again here. In fact, the response to the rising triangular impulse as shown in (Fig. 7c) is obtained from the Newmark explicit method with $\Delta t = 0.05$ s, except that a very small single time step of $\alpha(\Delta t)$, where $\alpha = 1$, 0.1 and 0.01 are taken, is performed right after the end of the impulse. Displacement errors for the response to the rising triangular impulse are plotted in Fig. 12. This figure reveals that the amplitude distortion decreases with the decrease of $\alpha$ and a very reliable solution is obtained from the use of $\alpha = 0.01$. Thus, an extra amplitude distortion caused by the discontinuity at the end of an impulse is identified and the feasibility of performing a very small single time step right after the end of the impulse to eliminate the discontinuity problem is confirmed without using the momentum equation of motion.

### 6.4. Example 4

In order to confirm that the momentum equation of motion is also applicable to overcome the discontinuity problem for nonlinear systems, the system used in example 1 is modified by changing the stiffness from a constant value to a function of displacement $u$ with the unit of N/m. In fact, the stiffness is taken to be

$$k = \pi^2(1 + u), \tag{15}$$

where $\pi^2$ is the initial stiffness, while the nonlinear stiffness is introduced after the system deforms and it is found to be $\pi^2 u$. Numerical results for the nonlinear system subject to the rising triangular impulse as shown in Fig. (7c) are plotted in Fig. 13. In this figure, the result obtained from the time step of $\Delta t = 0.0001$ s can be treated as an "**exact**" solution. It is clear that Scheme (a) using $\Delta t = 0.025$ or 0.05 s leads to very poor solutions, while those obtained from Scheme (b) are acceptable. This implies that the momentum equation of motion can also overcome the discontinuity problem for nonlinear systems.

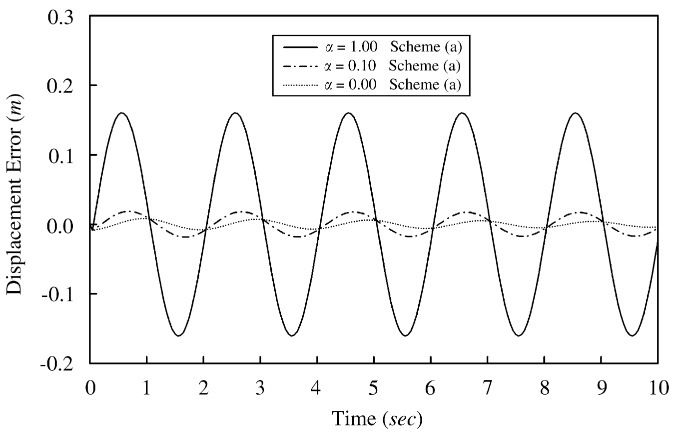


Fig. 12. Displacement error for responses to rising triangular impulse obtained from Newmark explicit method using Scheme (a) with different $\alpha$ values.

### 6.5. Example 5

To further confirm that the momentum equations of motion can overcome the discontinuity at the end of an impulse in the solution of a shock response for a multiple degree-of-freedom system, a 5-story shear-beam type structure subject to a triangular ground impulse is considered. The mass and stiffness for each floor are taken to be 1 kg and 100 N/m. The triangular ground impulse is in the form of ground acceleration and its time integral is in the form of ground velocity as shown in Fig. 14. The maximum ground acceleration and the duration of this impulse are assumed to be $100\,m/s^2$ and $t_0 = 0.01$ s, respectively. Apparently, the product of the ground acceleration and each story mass is the input external force for each story if the force equation of motion is used. Similarly, for the use of the momentum equation of motion, the product of the ground velocity and each story mass is the input external momentum for each story. The structural period and the ratio of $\Delta t/T_n$ for each mode of the 5-story shear-beam type structure are summarized in Table 2.

In Table 2, the natural frequency $\omega_n$ is in the unit of rad/s and the period $T_n$ is in the unit of seconds. This table shows that the use of $\Delta t = 0.0001$, 0.001 and 0.03 s for the step-by-step integration will introduce insignificant period distortion if the Newmark explicit method is used, since the ratios of $\Delta t/T_n$ are small for all five modes. Numerical results are plotted in Fig. 15, where the solutions computed from Scheme (a) using a time step of 0.0001 s are considered as "**exact**" solutions for comparison. Both Schemes (a) and (b) are used to obtain the responses to the triangular ground impulse. It is manifested from this figure that Scheme (a) with a

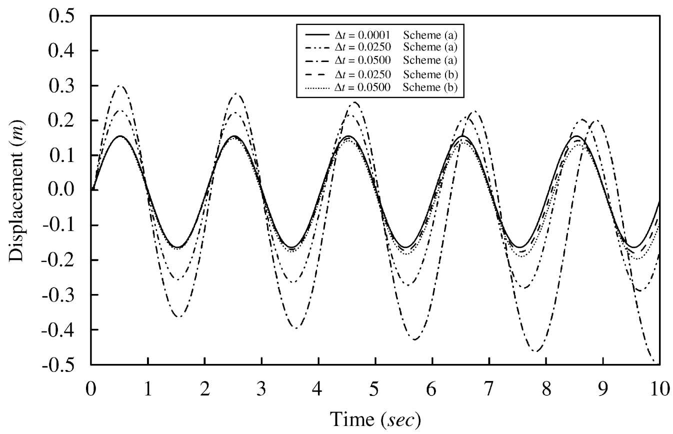


Fig. 13. Nonlinear responses to rising triangular impulse obtained from Newmark explicit method using both Schemes (a) and (b).

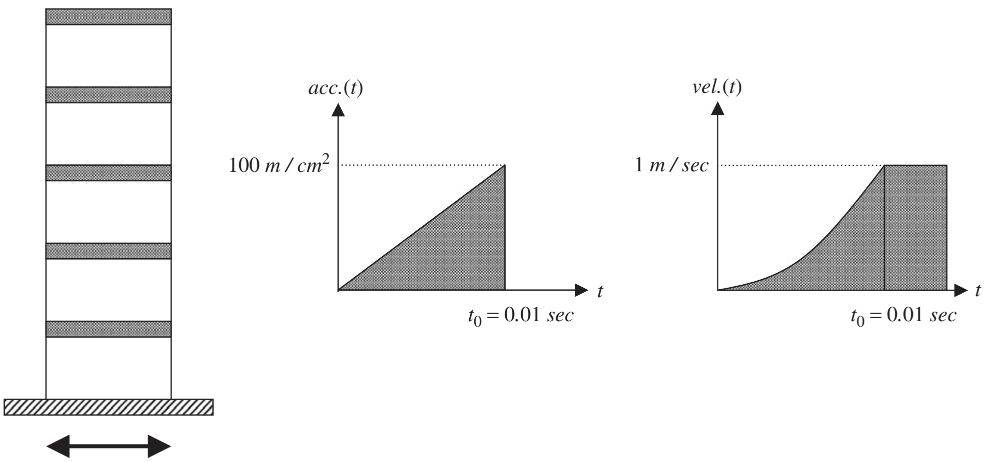


Fig. 14. Five-story shear-beam type structure subject to triangular ground impulse.

Table 2
List of $T_n$ and $\Delta t/T_n$

| | | | | | |
|---|---|---|---|---|---|
| $\omega_n$ | 2.846 | 8.308 | 13.10 | 16.83 | 19.19 |
| $T_n$ | 2.207 | 0.756 | 0.480 | 0.373 | 0.327 |
| $\frac{0.0001}{T_n}$ | $4.53 \times 10^{-5}$ | $1.32 \times 10^{-4}$ | $2.08 \times 10^{-4}$ | $2.68 \times 10^{-4}$ | $3.06 \times 10^{-4}$ |
| $\frac{0.001}{T_n}$ | $4.53 \times 10^{-4}$ | $1.32 \times 10^{-3}$ | $2.08 \times 10^{-3}$ | $2.68 \times 10^{-3}$ | $3.06 \times 10^{-3}$ |
| $\frac{0.03}{T_n}$ | $1.36 \times 10^{-2}$ | $3.97 \times 10^{-2}$ | $6.25 \times 10^{-2}$ | $8.04 \times 10^{-2}$ | $9.17 \times 10^{-2}$ |

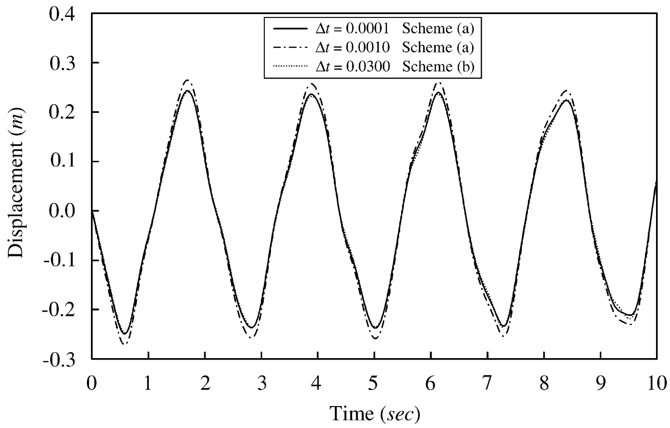


Fig. 15. Top story response to triangular ground impulse.

time step of 0.001 s, which is equal to $\frac{1}{10}t_0$, still cannot provide accurate solutions, while reliable results are obtained from Scheme (b) if a time step of 0.03 s is used, which is three times that of the loading duration. Thus, it is evident that the momentum equations of motion are superior to force equations of motion in the solution of the shock response to impulse. Apparently, the discontinuity at the end of the ground acceleration is responsible for the inaccurate solutions obtained from Scheme (a) with $\Delta t = 0.001$ s. In fact, for this case, the relative amplitude error is found to be $E^a_{\text{act}} = 0.09$ which is in good agreement with the analytical result estimated from Eq. (14) of $E_{\text{est}} = 0.1$. On the other hand, accurate results obtained from Scheme (b) with $\Delta t = 0.03$ s are due to the effective reflection of the external momentum-dependent effect and there is no discontinuity in the external momentum.

## 7. Conclusions

In this study, an analytical procedure is used to show that the shock response to an impulse obtained from the Newmark method will involve an extra amplitude distortion caused by the discontinuity at the end of the impulse. Furthermore, it is found that the relative amplitude error in the displacement response due to the discontinuity at the end of an impulse can be reliably estimated from the ratio of the area of the extra impulse over the area of the input impulse in the step-by-step integration. This is basically derived from the fact that the maximum displacement response to an impulse depends principally upon the magnitude of the applied impulse and is not strongly affected by the form of the loading impulse. Finally, it is shown that the momentum equation of motion, which is constructed from the dynamic equilibrium of momentums, can effectively overcome the difficulty caused by the discontinuity at the end of an impulse. This is because the discontinuity problem in dynamic loading will automatically disappear after the time integration of the impulse, which results in no discontinuity in the external momentum. All these analytical results are confirmed with numerical examples. The feasibility of using this technique for nonlinear systems is confirmed by numerical experiments. On the other hand, it is numerically shown that to conduct a very small time step immediately upon termination of applied impulse can effectively overcome the difficulty caused by load discontinuity.

## Acknowledgments

The author is grateful to acknowledge that the study is financially supported by the National Science Council, Taipei 106, Taiwan, Republic of China, under the Grant no. NSC-94-2211-E-027-011.

## References

[1] A.K. Chopra, *Dynamics of Structures*, international ed., Prentice Hall International Inc., Englewood Cliffs, NJ, 1997.
[2] R.W. Clough, J. Penzien, *Dynamics of Structures*, second ed., McGraw-Hill Inc., New York, 1993.
[3] S.Y. Chang, K.C. Tsai, K.C. Chen, Improved time integration for pseudodynamic tests, *Earthquake Engineering and Structural Dynamics* 27 (1998) 711–730.
[4] C.C. Chen, A.R. Robinson, Improved time-history analysis for structural dynamics calculations I: treatment of rapid variation of excitation and material nonlinearity, *Journal of Engineering Mechanics* 119 (12) (1993) 2496–2513.
[5] S.Y. Chang, Analytical study of the superiority of the momentum equations of motion for impulsive loads, *Computers and Structures* 79 (15) (2001) 1377–1394.
[6] N.M. Newmark, A method of computation for structural dynamics, *Journal of Engineering Mechanics Division, ASCE* 85 (1959) 67–94.
[7] T. Belytschko, T.J.R. Hughes, *Computational Methods for Transient Analysis*, Elsevier Science Publishers B.V., North-Holland, 1983.
[8] S.Y. Chang, Improved Dynamic Analysis for Linear and Nonlinear Systems, PhD Thesis, Department of Civil Engineering, University of Illinois, Urbana-Champaign, IL, USA.
[9] T.J.R. Hughes, *The Finite Element Method*, Prentice-Hall Inc., Englewood Cliffs, NJ, 1987.
[10] M. Zienkiewicz, *The Finite Element Method*, third ed., McGraw-Hill Book Co (UK) Ltd., New York, 1977.